Bubble Coalescence in Viscous Fluids

NOEL de NEVERS and JEN-LIANG WU

University of Utah, Salt Lake City, Utah

The gravity-driven coalescence of 1- to 2-cm. diameter air bubbles in glycerine and in water has been studied by high-speed cinematography. The resulting coalescence behavior can be correlated by a simple model which assumes that each bubble trails a wake, and that the bubble coalescing from below accelerates when it enters the wake of the preceding bubble and thus overtakes the first bubble. The predictions of the model are not significantly altered by different assumed wake configurations.

Bubble coalescence plays a significant role in determining the bubble-sized distribution and interfacial area in all sorts of gas-liquid contacting devices, and plays a dominant role in gas-liquid separating equipment. In a typical gas-sparged contactor or reactor, coalescence is detrimental because it decreases the surface area of the bubbles; in a separator it is desirable because it increases the size and hence the rise velocity of the bubbles.

In previous work two extreme cases of bubble coalescence have been studied. When the bubbles are very small (for example, 1 mm. or less in diameter) and their coalescence is driven by gravity in stagnant liquids, then the coalescence process proceeds by the gradual expulsion of the fluid between the coalescing bubbles (film thinning) much as it does for liquid droplets (*1*). At the other extreme, in agitated tanks in which a gas is fed into a liquid, there have been extensive studies of the bubble-size distribution, from which the statistical properties of the coalescence and breakup process can be inferred (*2*). For other conditions of coalescence our knowledge is meager (*5*).

One coalescing situation which is easy to observe and photograph is illustrated in Figure 1, in which bubbles rise in a chainlike fashion through a stagnant liquid. When the bubbles are spaced closely enough, one bubble will suddenly accelerate and overtake the preceding one.

It seems clear from visual observation that this behavior can be explained by assuming that the lower bubble moves into the wake of the upper bubble, which then allows the lower bubble to move more rapidly relative to fixed coordinates than it did previously. It does this because it is now encountering the upward-moving wake of the upper bubble, rather than encountering fluid at rest. To test this idea such coalescences were photographed, and their behavior compared with the predictions of a simple model based on the above explanation.

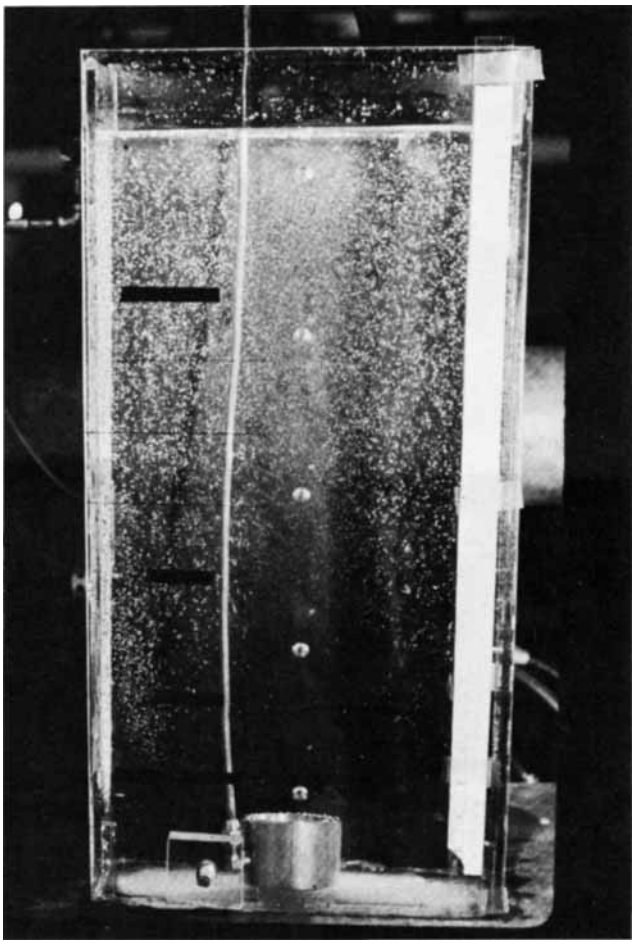

Fig. 1. Air bubbles about 1 cm. in diameter rising in chain formation in glycerine.

EXPERIMENTAL APPARATUS AND PROCEDURE

The bubbles were generated in a rectangular plexiglass tank, 4.5 in. by 12 in. by 24 in. The bubbles were released from a horizontal sparger with a circular hole 0.406 in. in diameter (Figure 1). The bubbles were of air; the fluids used were commercial grade glycerine and distilled water, to which a small amount of sodium ethyl xanthate was added to reduce surface tension and thus promote coalescence.

The bubbles were generated by forcing air through the sparger at such a rate that the bubbles formed at regular intervals and coalesced somewhere near the middle of the tank. The coalescence process was recorded with a Fastax Model WF17T rotating-prism movie camera, and the time-distance behavior of the coalescing bubbles calculated by measuring positions on the film with a Nikon Model 3C optical comparator. The details of the measurement process are discussed elsewhere (*3*).

WAKE-COALESCENCE MODEL

There are two variants on the basic model. Both variants have the following assumptions in common:

1. The two coalescing bubbles are assumed to be hemispherical in shape and equal in size, and rising in the same vertical line.
2. The only significant forces acting on the bubbles are the buoyant and drag forces. The drag force is assumed to

*J.-L. Wu is with the Colorado Research Foundation, Golden, Colorado.

be given by

$$F_d = C_D \rho \frac{V^2}{2} A_p \tag{1}$$

with C_D constant for a given bubble.

3. The density of the gas in the bubble is so small that the bubble's product of mass and acceleration is negligible. Thus the drag and buoyant forces are always equal and opposite.

4. Each bubble trails a wake of size and shape discussed below. When the lower bubble enters the wake of the upper bubble, its projected area (A_p) which is exposed to stagnant fluid is decreased by the amount of its projected area which is in the wake of the preceding bubble. This area in the wake of the preceding bubble makes no contribution to the drag on the lower bubble. Thus, as the projected area exposed to stagnant fluid decreases, the velocity relative to stagnant fluid must increase to keep the buoyant and drag forces equal.

5. Changes in pressure and temperature are negligible.

The first variant of the model assumes that the wake behind the bubble is conical, with dimensions as shown in Figure 2. From the similarity of the two right triangles ΔABC and ΔADE

$$\frac{\overline{BC}}{\overline{DE}} = \frac{\overline{BA}}{\overline{DA}} = \frac{\overline{BA}}{\overline{BA} - \overline{BH} - \overline{HD}}$$

that is,

$$\frac{R_1}{\alpha} = \frac{L_c}{L_c - x - h} \tag{2}$$

From the right triangle, ΔDFG

$$R_2^2 = \alpha^2 + (R - h)^2; \tag{3}$$

but it is assumed that $R_1 = R_2 = R$. When the following dimensionless quantities are defined

$$L_c^* = \frac{L_c}{R}, \quad h^* = \frac{h}{R}, \quad x^* = \frac{x}{R}, \quad \alpha^* = \frac{\alpha}{R} \tag{4}$$

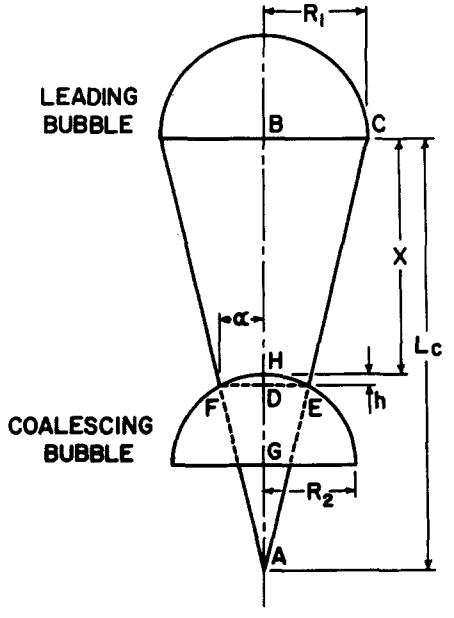

Fig. 2. Geometry of the conical wake variant of the model.

Equations (2) and (3) become

$$h^* = L_c^* (1 - \alpha^*) - x^* \tag{5}$$

$$1 = \alpha^{*2} + (1 - h^*)^2 \tag{6}$$

Insertion of Equation (5) into Equation (6) to eliminate h^* produces

$$(1 + L_c^{*2})\,\alpha^{*2} + 2L_c^*(1 - L_c^* + x^*)\,\alpha^* + (x^{*2} - 2L_c^* x^* + 2x^* + L_c^{*2} - 2L_c^*) = 0 \tag{7}$$

or

$$\alpha^* = \frac{(-L_c^* + L_c^{*2} - x^* L_c^*) \pm \sqrt{-x^* + (2L_c^* - 2)\,x^* + 2L_c^*}}{1 + L_c^{*2}} \tag{8}$$

Equating the drag and buoyant forces on the lower bubble, we have

$$\left(\frac{2}{3}\pi R^3\right) \rho g = C_D \rho \frac{V^2}{2} (R^2 - \alpha^2)\pi \tag{9}$$

For this form of the model if x is greater than L_c there is no coalescence because the lower bubble never enters the wake of the upper bubble. If x is less than L_c then we can let

$$V = V_t + \frac{dx}{dt} \tag{10}$$

and substitute this into Equation (9) to obtain

$$V_t + \frac{dx}{dt} = \left(\frac{4R^3 g}{3(R^2 - \alpha^2)C_D}\right)^{0.5} \tag{11}$$

With $t = Rt^*/V_t$ and the dimensionless quantities defined in Equation (4), Equation (11) can be written in dimensionless form as

$$1 + \frac{dx^*}{dt^*} = \left(\frac{4Rg}{3C_D V_t}\right)^{0.5} \frac{1}{(1 - \alpha^{*2})^{0.5}} \tag{12}$$

Since $V_t = (4Rg/3C_D)^{0.5}$, Equation (12) can be simplified to

$$\frac{dx^*}{dt^*} = \frac{1}{(1 - \alpha^{*2})^{0.5}} - 1 \tag{13}$$

Hence

$$t^* = \int_{L_c^*}^{x^*} \frac{dx^*}{\dfrac{1}{(1 - \alpha^{*2})^{0.5}} - 1} \tag{14}$$

To evaluate the integral in Equation (14) the value of α^* from Equation (8) is substituted in Equation (14). Then the integrand contains only x^* and L_c^*. Taking L_c^* as an unknown parameter which may be assumed constant (that is, assumed not to change during a given coalescence event) one may integrate Equation (14) numerically. This has been done using Simpson's rule for numerous values of L_c^* (3).

The second variant of the model assumes that the first bubble trails a wake in the form of an "exponential cone" whose radius decreases exponentially with distance (Figure 3), that is

$$y = R \cdot \exp^{-kx} \tag{15}$$

It follows that

$$\alpha = R \cdot \exp^{-k(x+h)}, \tag{16}$$

where k is a constant for exponential decay. Since h is small compared with the distance between the two coales-

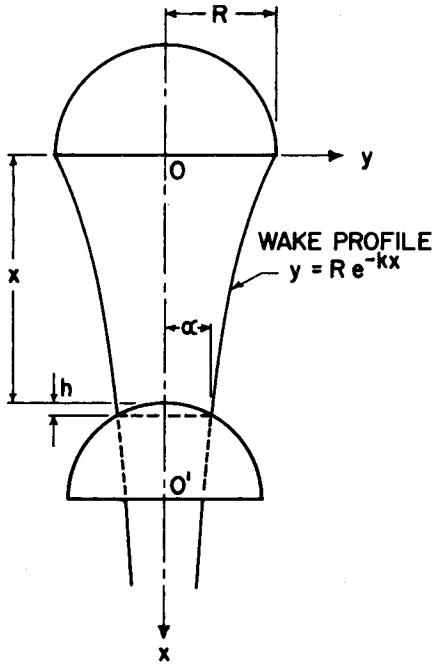

Fig. 3. Geometry of the exponential wake variant of the model.

cing bubbles, it is ignored for simplicity. Then

$$\alpha = R \cdot \exp^{-kx} \tag{17}$$

For this model there does not exist the region of bubble spacing in which the bubbles would never coalesce, as does in the conical wake variant of the model; the lower bubble is always in some part of the wake of the upper bubble and will eventually overtake it. Substituting Equation (17) into Equation (14) we have

$$t^* = \int_{x_0^*}^{x^*} \frac{dx^*}{\frac{1}{(1 - \exp^{-2kRx^*)^{0.5}}} - 1} \tag{18}$$

where x_0^* is the value of x^* at $t^* = 0$. Equation (18) has also been integrated numerically for various values of k (3).

A somewhat analogous approach for the case of droplets coalescence has been discussed by Mason (6).

EXPERIMENTAL RESULTS

Four coalescence events were selected from the high-speed films and measured on the optical comparator: two for the air-glycerine system and two for the air-water system. These events were selected over other events for measurement because they had the largest part of their coalescence occurring in the field of view of the camera. The pertinent parameters of these events are shown in Table 1. The radii listed are the actual maximum horizontal dimensions, rather than those one would calculate from the volume and the assumption of a hemispherical shape. The observed shapes are somewhat elongated in the vertical direction, compared to hemispheres. The calculated terminal velocities are based on the correlation of Harmathy (4), which assumes that each bubble is moving in a stagnant liquid. The observed bubble velocities are up to 30% faster than those listed here because the bubble flow induces a vertical upward flow in the region of the bubble chain.

Table 1. Experimental Conditions for Observed Coalescences

Coalescence event	1	2	3	4
Bubble fluid	Air	Air	Air	Air
Surrounding fluid	Glycerine	Glycerine	Water	Water
Bubble radius, cm.	0.76	0.87	0.54	0.53
Calculated terminal velocity (cm./sec.) relative to fluid according to reference 4	25.8	26.8	24.8	24.6
Observed terminal velocity relative to container	28.5	29.6	33.6	32.4

Figure 4 shows the observed t^*–x^* behavior of the first coalescence event, comparing the experimentally observed position-time points with the curves from the two variants of the model which gave the best fit of the data. Figures 5, 6, and 7 show similar comparisons for the second, third, and fourth coalescence events.

In comparing theoretical curves with the experimental data, one has available as a fitting constant one free variable in each of the models (k in the exponential wake model and L_c^* in the conical wake model). The choice of value for these constants allows one to match the data with one of a family of similar curves. The choice of constant does not allow one to change the shape of the curves, but only the relative position on the t^*–x^* plane. For both glycerine coalescences, the best fits were obtained with $L_c^* = 7$ and $k = 0.24$ cm.$^{-1}$. For both water coalescences the best fits were obtained with $L_c^* = 10$ and $k = 0.28$ cm.$^{-1}$.

DISCUSSION

For the first two events (coalescence in glycerine) there is very little scatter of the experimental data, and the data

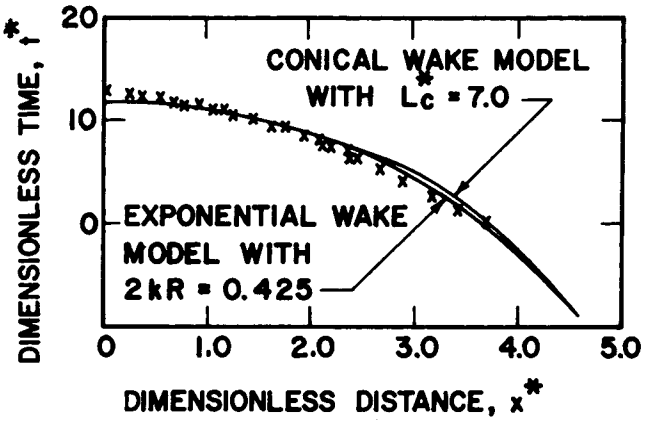

Fig. 4. Comparison of the experimental data with the theoretical curves for the first glycerine coalescene.

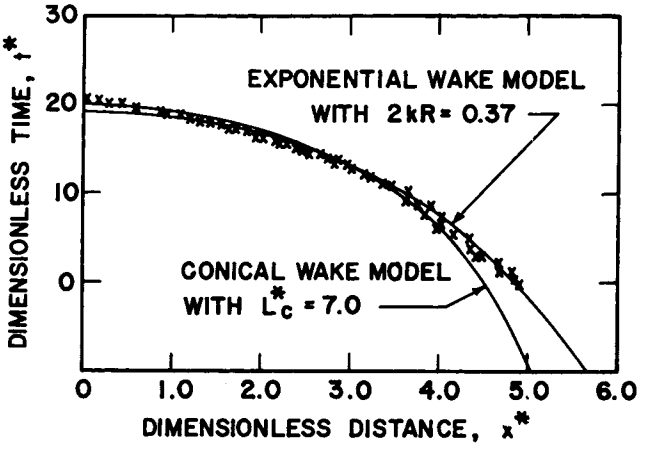

Fig. 5. Comparison of the experimental data with the theoretical curves for the second glycerine coalescence.

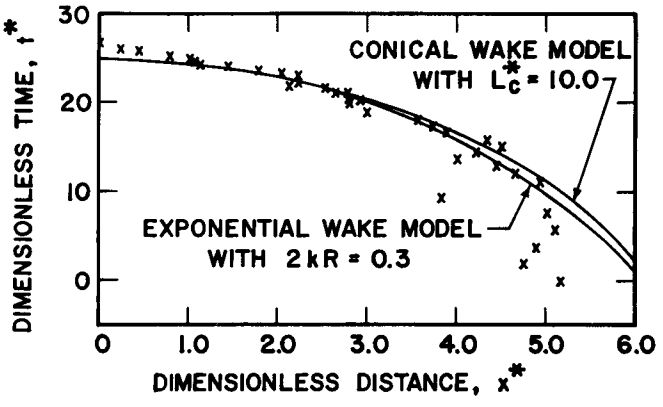

Fig. 6. Comparison of the experimental data with the theoretical curves for the first water coalescence.

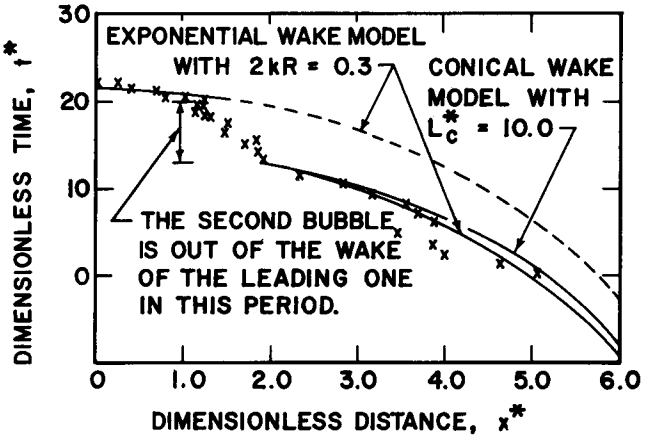

Fig. 7. Comparison of the experimental data with the theoretical curves for the second water coalescence.

agree well with both variants of the proposed model, to a distance of about $x^* = 4$. For larger distances it appears that the exponential wake model gives a better agreement with the data, which is plausible.

For all four events the experimental points lie above the theoretical curves as x^* approaches zero. According to the models the relative velocity must become infinite as x^* becomes zero. However as x^* becomes very small the viscous resistance of the fluid between the bubbles becomes significant and causes the velocity of approach to be less than one calculates by the model which ignores this resistance. Thus this failure of the model at the very end of the coalescence process is not surprising.

For the two coalescences in water there is considerably more scatter of the data than for the glycerine coalescences because of the shape oscillation of the bubbles. Visually it is clear that the water bubbles have a sidewise oscillatory motion in addition to their vertical motion, and that their shape changes in an oscillatory fashion. Neither of these phenomena is observed in the glycerine. These motions and the changing shape of the bubble make measurement of the positions more difficult, and lead to the experimental scatter shown in Figures 6 and 7. For Figure 6 the experimental data out to an x^* of 5 can be satisfactorily represented by either variant of the model. However for Figure 7 it is clear that no single curve from the model can represent these data. One plausible explanation of the data shown in Figure 7 is that during the time period from $t^* = 12$ to $t^* = 20$, the lower bubble was partly out of the wake of the upper bubble, and hence was encountering more stagnant fluid than the model predicts. To test this hypothesis, the horizontal positions of the two coalescing bubbles for this event were measured from the film. As shown in Figure 8 for part of the period in which the lower bubble was believed to be at least partly out of the wake of the upper bubble, its lateral displacement relative to the upper bubble is greater than the radius of the upper bubble. To settle this question completely it would be necessary to have a three-dimensional picture of the event (which could be obtained on one film with mirrors) and a description of the shape of the wake of the preceding bubble. In the air-glycerine system in which there is no visible side-to-side motion or shape oscillation it seems safe to assume that the wake is vertical. In this case, where there is pronounced side-to-side motion such an assumption is not as certain.

Two observed facts which are not shown by the simple model used here are first that the lower bubble becomes longer and thinner just before coalescing (Figure 9), and second that the upper bubble increases slightly in upward velocity just before coalescence. Both of these results are

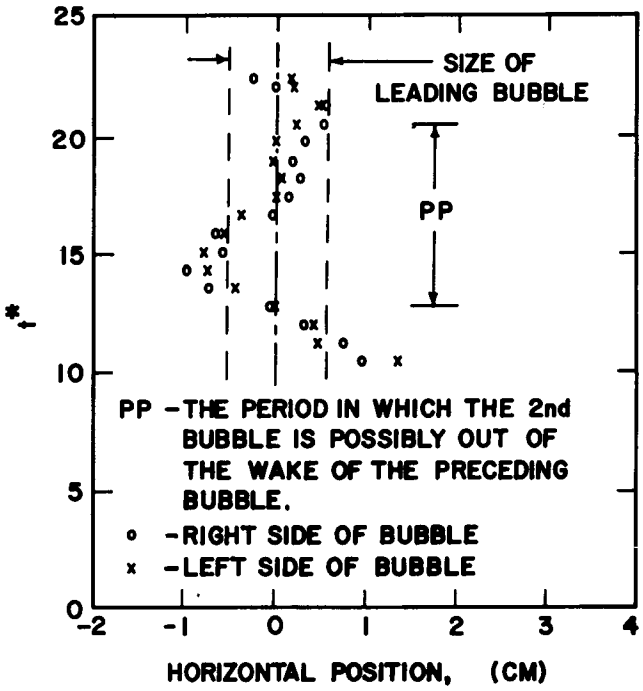

Fig. 8. Horizontal position of the lower bubble relative to that of the upper bubble for the second water coalescence.

Fig. 9. Lengthening of the lower bubble just before coalescence. This is at the terminal stage of coalescence event No. 2. In the earlier stages the two bubbles were practically identical in size and shape.

logically explained in terms of the physical model proposed, but neither of them is covered by the simple mathematics used.

CONCLUSIONS

1. Bubbles of diameter of 1 to 2 cm. formed serially at spacings of 3 to 4 cm. at a single circular 0.406 in. in diameter orifice rise in a chainlike fashion in stagnant glycerine or water, and frequently coalesce within 60 cm. of the orifice. In distilled water the bubbles frequently collide without coalescing: a small amount of sodium ethyl xanthate added to the water causes them to coalesce when they collide.
2. This coalescence can be described reasonably well by a wake-coalescence model, which assumes that the only significant forces acting on the lower bubble are its buoyant force and the inertia drag force, which decreases as it enters the wake of the preceding bubble.
3. The experimental results seem to agree about equally well with the predictions of the model, based on two different assumed wake geometries. This indicates that the assumed shape of the wake is not particularly significant.
4. The model incorrectly predicts a greater rate of increase in relative velocity in the last stages of the coalescence process than is experimentally observed.

ACKNOWLEDGMENT

This work was partially supported by NSF Grant GK-80.

NOTATION

A_p = projected area, sq. ft.
C_D = drag coefficient
F_d = drag force, lb.$_f$
g = acceleration of gravity, ft./sec.^{2}
h = geometric quantity as defined in Figure 2, ft.
h^* = h/R
k = exponential decay constant, Equation (17), 1/ft.
L_c = cone height as defined in Figure 2, ft.
L_c^* = L_c/R
R = bubble radius, ft.
t = time, sec.
t^* = tV_t/R
t_c^* = t^* at coalescence
V = velocity, ft./sec.
V_r = relative velocity between two coalescing bubbles, ft./sec.
V_t = terminal velocity of a single bubble in a stagnant fluid calculated according to reference *4*, ft./sec.
x = vertical distance between bubbles, ft.
x^* = x/R

Greek Letters

α = geometrical quantity as defined in Figure 2, ft.
α^* = α/R
ρ = liquid density, lb.$_m$/cu. ft.

LITERATURE CITED

1. MacKay, G. D. M., and S. G. Mason, *Can. J. Chem. Eng.*, **41**, 203–212 (1963).
2. Calderbank, P. H., in "Mixing, Theory and Practice," V. W. Uhl and J. B. Gray, eds., Vol. 2, p. 18 et seq., Academic Press, New York (1967).
3. Wu, Jen-Liang, M.S. thesis, Univ. Utah, Salt Lake City (1969).
4. Harmathy, T. Z., *AIChE J.*, **6**, 281 (1960).
5. Calderbank, P. H., M. B. Moo-Young, and R. Bibby, *Proc. Third European Symp. Chem. Reaction Eng.*, Amsterdam, 15–17, Sept. 1964, Suppl. *Chem. Eng. Sci.*, **20** (1965).
6. Mason, B. J., *Endeavor*, **23**, 136 (1964).

Manuscript received March 27, 1969; revision received June 26, 1969; paper accepted June 28, 1969.

A Thermodynamic Consistency Test for Adsorption from Binary Liquid Mixtures on Solids

S. SIRCAR and A. L. MYERS

University of Pennsylvania, Philadelphia, Pennsylvania

A thermodynamic consistency test for adsorption from binary liquid mixtures is derived using the Gibbs equation for adsorption. Adsorption data for the liquid mixture pairs A-*B*, A-C, and *B*-C on the same adsorbent must be thermodynamically consistent. The consistency test is applied to experimental data for adsorption from the binary liquid mixtures benzene-cyclohexane, benzene-*n*-heptane and cyclohexane-*n*-heptane on silica gel at 30°C.

The recent monograph by Kipling (*6*) provides a review of research on adsorption at the liquid-solid interface. Kipling points out that "The fundamental investigation of adsorption proceeded only slowly, in spite of its technological importance." There are at least two reasons for slow progress in the field of adsorption from liquids. First, there is a basic difference in the treatment of adsorption at the liquid-solid interface and adsorption at the gas-solid interface. A thorough explanation of the problem is given in Chapter II of the book by Defay, Prigogine, Bellemans,